J Mater Sci (2008) 43:3782–3791
DOI 10.1007/s10853-007-2128-2

Grain boundary reorientation in copper

V. Randle · Y. Hu · M. Coleman

Received: 23 May 2007 / Accepted: 23 August 2007 / Published online: 6 March 2008

Abstract The present route to grain boundary engineering (GBE) is usually based on multiple annealing twinning which can only be applied to a certain subset of materials, namely those that twin prolifically. A more general approach has been highlighted recently, following experimental evidence that certain boundary planes in iron bicrystals are 'special', and that this classification is not based on misorientation. It was suggested that, under suitable conditions, individual interfaces could reorient the most energetically advantageous orientations. This approach concurs with a similar concept of 'grain boundary plane engineering', proposed previously. In the present article we explore this concept and report the effect of long duration, low temperature annealing on the distribution of boundary misorientation and planes in copper. The new findings give support to the possibility of grain boundary structure optimisation via controlled annealing. To have established that grain boundary plane reorientation is feasible opens up new avenues and challenges in the field of grain boundary research. This could have significant impact both scientifically in terms of understanding grain boundary structure and technologically in the field of GBE.

Introduction

The most important component of polycrystalline materials is the internal interface (grain boundary) network. The properties of grain boundaries are different from those of the lattice. For example, grain boundary diffusion is much more rapid than its counterpart in the lattice. Grain boundaries are not uniform with respect to their properties; properties such as energy or mobility can vary enormously depending on grain boundary structure. Whereas this fact has been known for a long time, it is only in recent years that attempts have been made to understand in detail the relationship between boundary structure and properties, and hence to exploit it to improve material performance. This endeavour has come to be known as 'grain boundary engineering', GBE [1, 2].

Most attempts to understand the relationship between grain boundary structure and properties have focussed on face-centred cubic materials which form annealing twins readily. There are several illustrative examples associated with the GBE initiative, where characterisation of boundaries has remained very largely misorientation-based [e.g., 3]. This means that of the five parameters required to characterise an interface, only three are used. Although this practice has the advantage of experimental simplicity, it ignores the orientation of the grain boundary plane (the remaining two parameters). Yet a growing body of evidence is indicating that 'special' (i.e., good) boundary properties depend crucially on the orientation of the boundary plane. For example, a recent molecular dynamics simulation has shown that in aluminium grain boundary mobility increases as the plane deviates from {111} [4]. This was shown to have particular relevance to $\Sigma 3$ boundaries (found to be either very high or very low mobility) and $\Sigma 7$ boundaries (found to have rather low mobility), where the Σ notation refers to a misorientation characterisation in the coincidence site lattice (CSL) notation. Other work, based on both computer simulation and high-resolution electron microscopy, has also firmly established the role of the boundary plane. It is shown that the grain boundary energy depends on the tilt and twist

V. Randle (✉) · Y. Hu · M. Coleman
Materials Research Centre, School of Engineering, University of Wales Swansea, Swansea SA2 8PP, UK
e-mail: v.randle@swansea.ac.uk

characteristics, and that both symmetrical and asymmetrical tilt boundaries have lower than average energy [5, 6].

Given the importance of the boundary plane in influencing properties, it makes sense both to measure orientation distributions of boundary planes in polycrystals, and to attempt to modify the plane population towards lower energy configurations. This aspiration was recognised some years ago, when it was shown that a long duration anneal at $0.6T_m$ permitted Σ3 boundaries in polycrystalline copper to reorient and approach more closely the 'special' {111} planes. At the time, this was recognised as a potential route to 'in-situ grain boundary plane engineering' [7]. Recently this idea has been proposed again, following an experimental evidence that certain boundary planes in iron bicrystals are 'special', and that this classification is not based on misorientation [8]. It was demonstrated theoretically that under suitable conditions individual interfaces could reorient to the most energetically advantageous boundary plane orientations, without grain rotation and alterations in either texture or boundary misorientation, hence potentially providing a general route for GBE. In the present work, therefore, we build upon these previous demonstrations of the feasibility of boundary plane reorientation, to examine the phenomenon in more detail.

Recently it has become possible to measure all five parameters grain boundary parameters (i.e., misorientation and boundary plane) for huge sample populations of boundaries, by use of a technology based on electron backscatter diffraction, EBSD [9]. This is a landmark experimental advance because it delivers new, hitherto inaccessible, insights into the grain boundary network structure, which in turn is impacting on our understanding of why some boundaries are 'special' and others are not. Only certain ceramic systems, e.g., MgO [10] and some metallic systems [11, 12] have to be examined in any detail.

The five-parameter analysis will be used in the present work to assess and to analyse boundary plane reorientation in commercially pure copper after long duration annealing at 500 °C. The annealing schedule of the current experiment is a duplicate of that used previously to reorient or 'fine tune' Σ3 boundaries in copper [7], where 'Σ3' refers to boundaries which have a misorientation of 60°/<111>. In the previous work, only Σ3 boundaries were examined, and the sample population was relatively small, 200 Σ3s after annealing. In the present work, more than 160,000 boundary segments from each of a reference and a heat-treated specimen will be analysed in depth, to include *all* interfaces, not Σ3s alone.

Experimental

Commercially pure, lightly deformed copper specimens were annealed at 700 °C for 90 min in air to ensure a recrystallised microstructure with a uniform grain size. This will be called the 'reference' sample. The specimen was metallographically prepared in the normal way, followed by polishing in a silica slurry and then etching in modified Livingston's reagent. A Channel 5 EBSD system from HKL Technology, interfaced to a Philips XL30 SEM, was used to acquire many high-resolution orientation maps encompassing approximately 40,000 grains, which equated to more than 160,000 boundary segments. A step size of 1 μm was used to obtain the maps. Grain size, microtexture and grain boundary misorientation parameters were obtained using HKL Technology's Tango and Mambo software suites. The 'five-parameter' analysis software was then used to identify and to reconstruct grain boundary segments, by use of a boundary reconstruction algorithm in the TSL software package to obtain the distribution of both misorientations and boundary planes. Many random boundaries were curved, which the boundary reconstruction algorithm takes account of by appropriate segmentation of the boundary into tangential sections, according to user-defined limits. The procedures for this and the five-parameter analysis are described in detail elsewhere [9, 10]. The Brandon criterion [13] was used to classify $\Sigma 3^n$ boundaries with $n \leq 3$, i.e., Σ3, Σ9 and Σ27, as a fraction of total boundary length. The accuracy of a misorientation measurement obtained by EBSD is 0.5°. Grain boundary distributions as determined by the five-parameter software are presented in Multiples of a Random Distribution (MRD) and the resolution of the distribution is approximately 10°. Some of the specimens were further annealed in air for 97 h at $0.6T_m$ (500 °C). This will be called the 'annealed' sample. The EBSD data collection and five-parameter analysis was repeated on these specimens.

Results

The average grain size was 18 μm and 19 μm before and after the long duration anneal, respectively. The small increase in average grain size was due to anomalous grain growth in a few regions whereas in the majority of the regions the grain size had remained static. Figure 1 illustrates a region in the annealed specimen where both large and small grains are present. The microtexture was random in both cases, which was a consequence of the high level of annealing twinning. The proportion of interface length that was Σ3, Σ9 and Σ27 was 61%, 6% and 3% respectively in both the reference sample and the annealed sample. In terms of number fractions, the number of interfaces that were Σ3, Σ9 and Σ27 were approximately 42%, 10% and 6%, respectively. These statistics were extracted from regions of specimen where grain growth was absent. In the

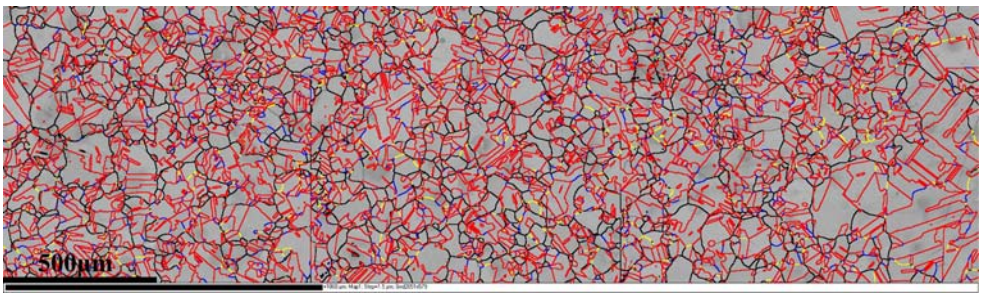

Fig. 1 Orientation map of the annealed copper sample, showing some anomalous grain growth on the right-hand side. Σ3, Σ9, Σ27, low angle and general boundaries are coloured red, blue, yellow, light grey and black respectively

anomalous grain regions, the length fraction of Σ3 had increased to 65%. The data indicate that in the static grains, the $\Sigma 3^n$ fractions had not increased as a consequence of long duration annealing, which further illustrates that there was no sustained grain boundary migration and no newly generated annealing twins except, as illustrated in Fig. 1, in regions of anomalous grain growth. The Σ9 and Σ27 fractions are higher than those expected in a random distribution because there is a high fraction of Σ3 boundaries, and where two Σ3s conjoin a Σ9 boundary results.

The distribution of grain boundary planes is reported as 'multiples of a random distribution', MRD, on a stereographic projection. Figure 2a and b shows the entire distribution of planes for the reference and annealed samples respectively. There are maxima at {111} and minima at {100}. The maxima are mainly the result of the presence of Σ3 annealing twins, which are on {111}. The maximum MRD value for the reference and annealed sampled are 6.8 and 5.8, respectively, i.e., there is a reduction in the proportion of {111} after annealing. If all Σ3s are removed from both datasets, there is still a small maximum at {111}, 1.4 MRD for both samples. This result is consistent with previous five-parameter measurements on aluminium [11] and brass [12].

Aspects of the five-parameter distribution were examined in detail via observation of the plane distributions for specific misorientations categorised according to low index misorientation axes <100>, <111> and <110>. In each of the datasets, there were almost no misorientations on <100>, and approximately 4% of misorientation length was on <111>, excluding Σ3s. For the [111] misorientation axis the trend for boundary planes was for them to be (111) twists. The proximity to exact (111) was greater for the annealed than for the reference sample. This is illustrated on Fig. 3a and b for the reference and annealed samples, respectively, using the 50°/[111] misorientation angle/axis pair as an example. (Note that where misorientation statistics alone are quoted, it is appropriate to refer to a non-specific misorientation axis, i.e., <uvw>. However, for five-parameter analysis of a particular misorientation subset, whereas all misorientations in the <uvw> family are included in the data processing, all misorientations are expressed as one specific axis [uvw] for representation.) It can be seen in Fig. 3 that both the MRD values have increased from 1.5 to 4.1 and that the angular spread about the exact (111) plane has diminished as a consequence of annealing. Other misorientation angles about [111] show the same trend.

Approximately 12% of total boundary length was misoriented on <110>, not including Σ3. Σ3 has a solution of 70.53°/<110> which is symmetry-equivalent to the disorientation solution of 60°/<111> (where 'disorientation' refers to the lowest angle solution of a misorientation). The <110> misorientation axis subset of the boundary population includes Σ9, 38.94°/<110>, and Σ27a, 31.59°/<110>. Figure 4 shows the distribution on the [110] misorientation axis over the angle range from 10° to 60°.

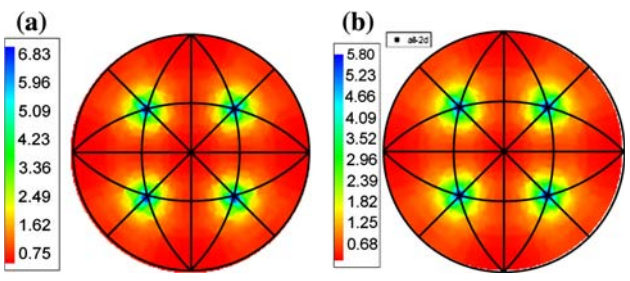

Fig. 2 Distribution of all boundary planes in [001] stereographic projection expressed as multiples of a random distribution, MRD. (**a**) reference sample (**b**) annealed sample

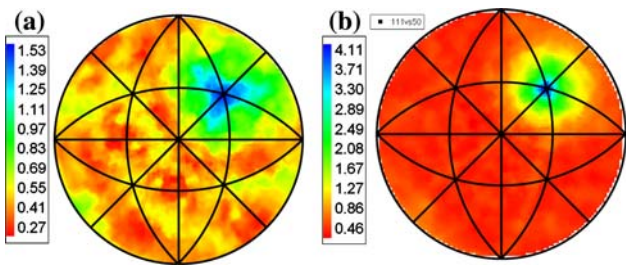

Fig. 3 Distribution of boundary planes in [001] stereographic projection expressed as multiples of a random distribution, MRD, in the 50°/[111] misorientation section. (**a**) reference sample (**b**) annealed sample

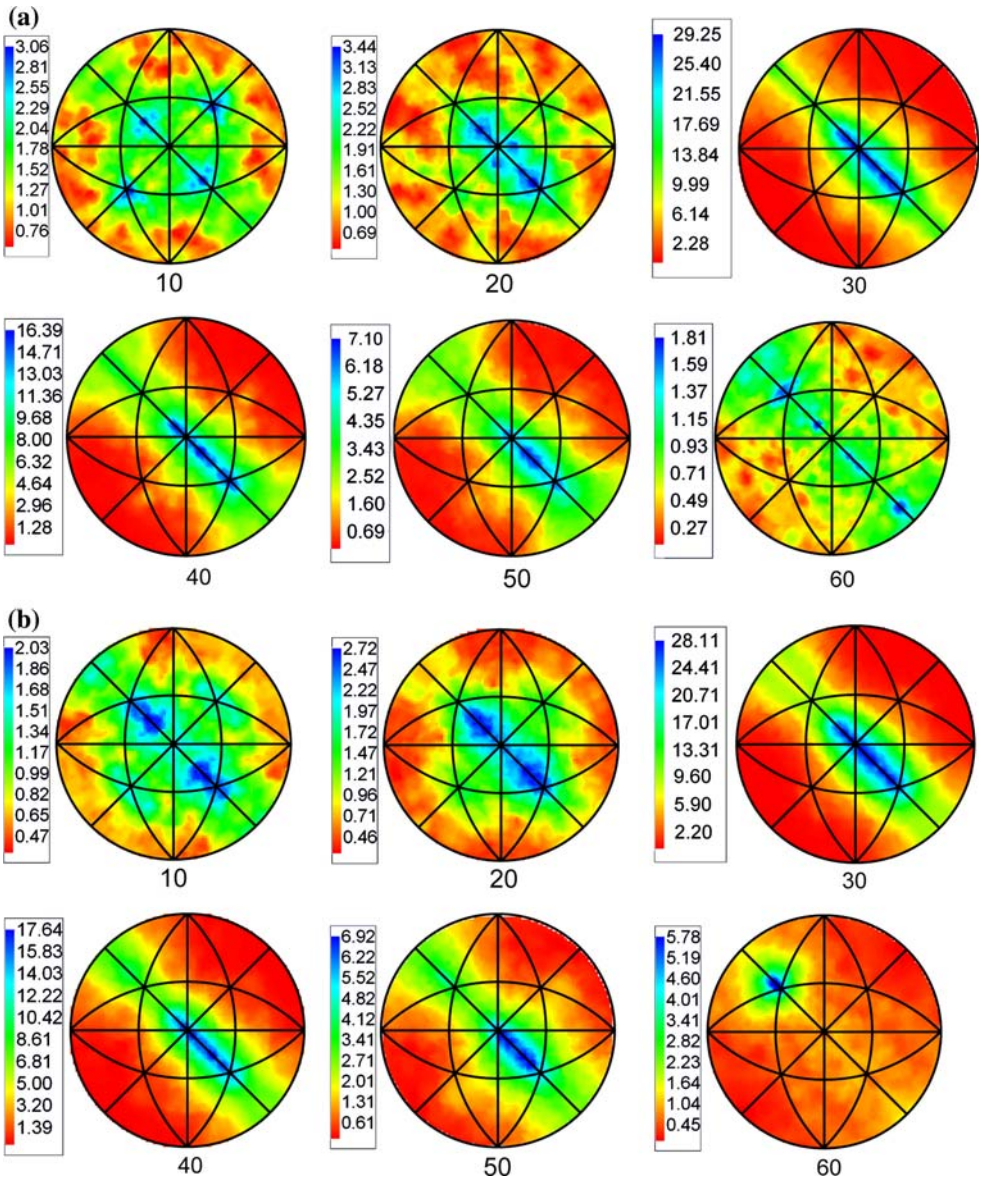

Fig. 4 Distribution of boundary planes in [001] stereographic projection expressed as multiples of a random distribution, MRD, in 10–60°/[110] misorientation sections, 10° misorientation angle increments as labelled. The position of the [110] misorientation axis is marked on the first section. (**a**) reference sample (**b**) annealed sample

The striking feature of the plane distributions on the [110] misorientation axis is that the density distribution is clustered on or around the [110] zone, i.e., the boundaries are tilt or near-tilt. The presence of several, often overlapping, peaks on the [110] zone indicates the presence of asymmetric tilt boundaries, ATGBs. For all cases, the maximum MRD values are several times higher than random. In particular in the range 30–50°, the maximum MRD values are very high (6.9–29.3). This range includes the Σ9 and the Σ27a misorientation.

After annealing, in every angle range the plane density is concentrated more closely on the [110] zone than before annealing. This is evident both in terms of the width of the spread about the [110] zone, which is greater in the reference sample, and the presence of off-zone peaks in the reference sample which are absent in the annealed sample. An example is seen in the 20°/[110] section. For some angle sections, there are also changes in the distribution of maxima along the [110] zone as a consequence of annealing. In other words, the boundary planes represented have changed. In particular, for the 60°/[110] misorientation the distribution of planes has changed sharply as a consequence of annealing, from having several maxima along the [110] zone to occupying a single maximum vicinal to (111). The MRD values have also increased from 1.8 in the reference specimen to 5.8 in the annealed specimen. For misorientations up to 50°, the distribution is spread over a wide range of planes whereas for misorientations greater than 50° the distribution is concentrated into less planes.

The Σ27 boundaries were split almost equally between Σ27a and Σ27b in both samples when the Brandon criterion (2.9° tolerance) is used for classification. However, if a 5° tolerance is used, there is twice as much Σ27a length as Σ27b length. The disorientation for Σ27b is 35.42°/<210>. Figure 5a and b shows the distribution for Σ27b in both the reference and annealed samples, respectively. Even though the disorientation axis is not [110], the plane distribution is still aligned close to [110] zone planes.

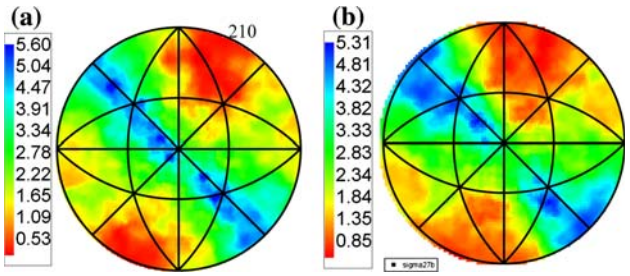

Fig. 5 Distribution of boundary planes in [001] stereographic projection expressed as multiples of a random distribution, MRD, for the Σ27b misorientation, 35.42°/[210]. (**a**) reference sample (**b**) annealed sample. The location of [210] is marked on (**a**)

In Fig. 6, the Σ3 boundary population is plotted, viewed as the misorientation 70.53°/[110] rather than the disorientation 60°/[111], so that the distribution with respect to the [110] tilt zone is revealed. For better precision, the distributions are shown as line contours rather than colours. There is a very strong maximum centred on (−111) for both specimens, with MRD values of 1,807 for the reference specimen and 1,515 for the annealed specimen. These maxima correspond to the presence of a high-length fraction of coherent twin boundaries. There is a reduction in the length fraction of coherent twins after annealing, which concurs with the reduced maximum after annealing seen in Fig. 2.

Discussion

A summary of the changes in the grain boundary plane distribution brought about by the long anneal is

- A reduction in the proportion of Σ3 length which was on {111} planes.

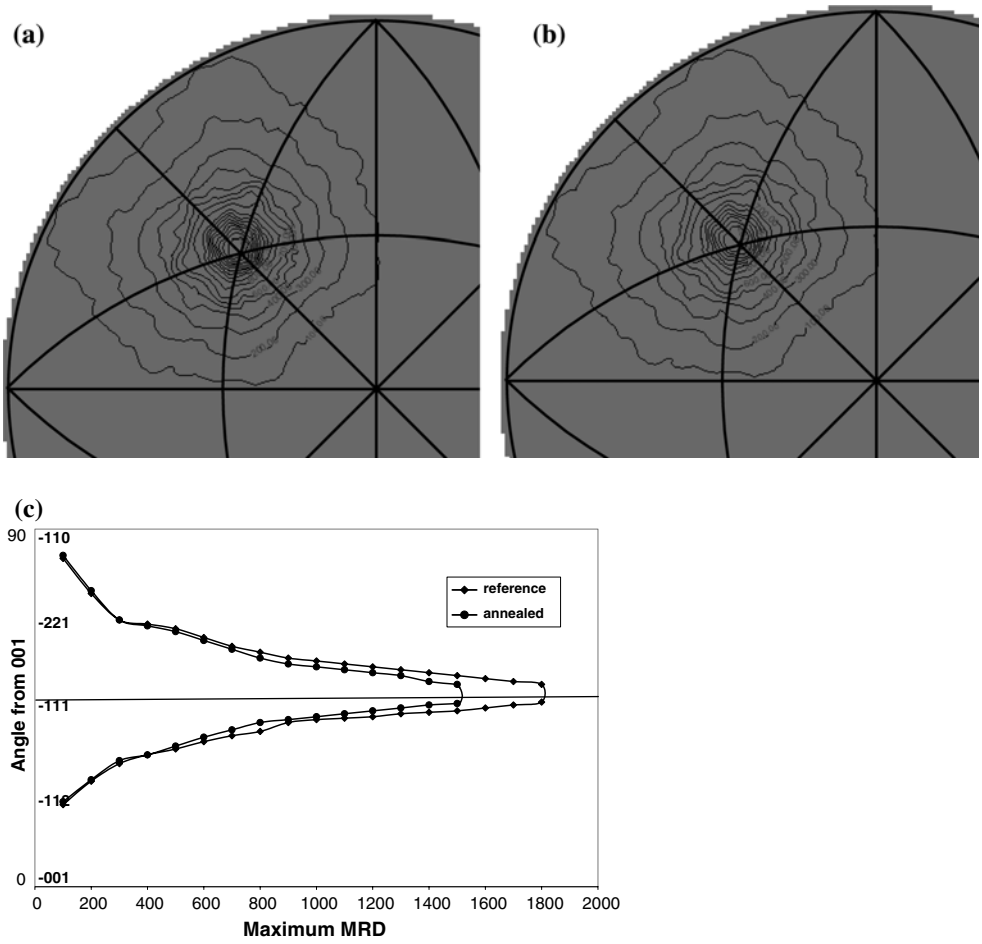

Fig. 6 Distribution of boundary planes in [001] stereographic projection expressed as multiples of a random distribution, MRD, for the Σ3 misorientation expressed as 70.53°/[110]. The distribution is shown as line contours in increments of 100× MRD in one-quarter of the stereogram. (**a**) reference sample (**b**) annealed sample. (**c**) Maximum MRD as a function of angular distance along the [110] zone. The location of some planes is marked, and the location of (−111) is additionally marked with a line

- For boundaries misoriented on <110> (apart from Σ3) a larger proportion of tilt boundaries or near-tilt and the distribution of planes on the tilt zone changed.
- A small increase in the proportion of {111} twist boundaries.

We will first discuss the population of Σ3 boundaries, which comprises nearly two-thirds of the total interface length. Figure 6a and b provide a detailed view of the density contours around the (−111) peak for Σ3, and Fig. 6c shows the maximum MRD as a function of angular distance along the [110] zone. Figure 6 shows that for both samples there is spread about the (−111) peak, with the MRD density falling off steeply for the first approximately 6° deviation from (−111). The MRD in the reference sample decreases from 1,800 to 900 in this range, whereas there are fewer exact (−111) planes in the annealed sample and here the density decreases from 1,500 to 900. For greater deviations from (−111) than 6°, the rate of MRD density reduction with increasing angular deviation from (−111) is slower. In this latter region, the form of the curves is almost identical for both samples.

The tail of maximum MRD density indicates the presence of planes other than (−111) within the Σ3 category. These can be described as 'vicinal-to-{111}' if they are a few degrees away from the ideal (−111) plane, and ATGBs if they are close to the [110] zone. It is known from several previous investigations which had identified the planes of individual boundaries that the Σ3 population in fcc metals following annealing twinning comprises a range of boundary planes, many of which are ATGBs on the <110> zone. For example, {113}/{335} and {117}/{155} have been reported in copper and aluminium, respectively [14, 15]. In brass, 65% of Σ3s had planes that were either vicinal-to-{111} or exact {111}. Some other Σ3 ATGBs were recorded, namely {211}/{552}, {221}/{744}, {511}/{111} and {772}/{10,11} [16].

Table 1 shows the planes of Σ3 boundaries recorded for a copper specimen which underwent exactly the same annealing schedule as that reported here [7]. In the data from that work 68% of the Σ3s were {111}, and 21% were classed as vicinal-to-{111} on the <110> zone (up to 10° displaced from {111}). Even though the previous investigation only measured 200 Σ3 boundaries, they show the same features as the present data provide substantiation for our interpretation of the spread around the (−111) peak to be the presence of ATGBS and, where the density decays sharply over approximately the first 6° away from (−111), the presence of vicinal-to-{111} boundaries. The values of grain boundary free energy shown in the table indicate that increasing boundary energy correlates with increasing deviation from {111} [17]. In the present data, the decay of the peak with angular displacement from (−111) accords

Table 1 Calculated boundary free energy for various Σ3 boundary planes in copper and previous experimental data

Boundary planes	Angle from {111}	Experimentally observed number of boundaries (previous data from copper annealed 540 °C/97h, [7])	Boundary free energy (Jm^{-2}), [17]
111/111	0	66	0.01
23,17,17/775	8.5	17	0.12
332/10,77	10	4	0.14
774/855	13.3	0	0.19
221/744	15.8	0	0.22
552/211	19.5	3	0.26
441/522	25.2	0	0.32
771/311	29.5	0	0.36
110/411	35.2	0	0.41
881/11,22	40.3	0	0.45
772/10,11	46.7	0	0.49
221/100	54.7	0	0.56
111/511	70.5	0	0.61

with the concomitant increase in boundary energy as shown in the table. It has been recognised previously that on a microscopic scale vicinal-to-{111} Σ3s are composed of long terraces of {111} interspersed with short steps of higher index planes [7]. The density of the steps increases with the deviation from {111}.

Although some of the Σ3 length is coherent twin boundary, as recognised by the strong maximum at {111}, it was initially puzzling that the density of {111} planes decreased from a maximum MRD of 1807 before annealing to a maximum MRD of 1,500 after annealing. This was an unexpected result. It has been shown previously that twins can be annihilated during normal grain growth when grain boundaries sweep through the microstructure [18], but this is not a feasible explanation in the present case because there has been no sustained grain boundary migration, apart from the few regions of anomalous grain growth.

If the length fraction of Σ3s has remained the same during annealing and yet the density of {111} planes has decreased, the implication is that the proportion of incoherent Σ3s must have increased. This could come about as a two-stage process, as follows. In direct contrast to coherent Σ3s, some incoherent Σ3s, or incoherent segments on Σ3s, have very high mobility. Therefore these intra-grain interfaces migrated during the long anneal whereas boundaries in the grain boundary network remained static. When different Σ3 boundaries within the same grain encounter one another during migration, a Σ9 boundary results according to the reaction Σ3 + Σ3 → Σ9 (stage 1). This Σ9 boundary may

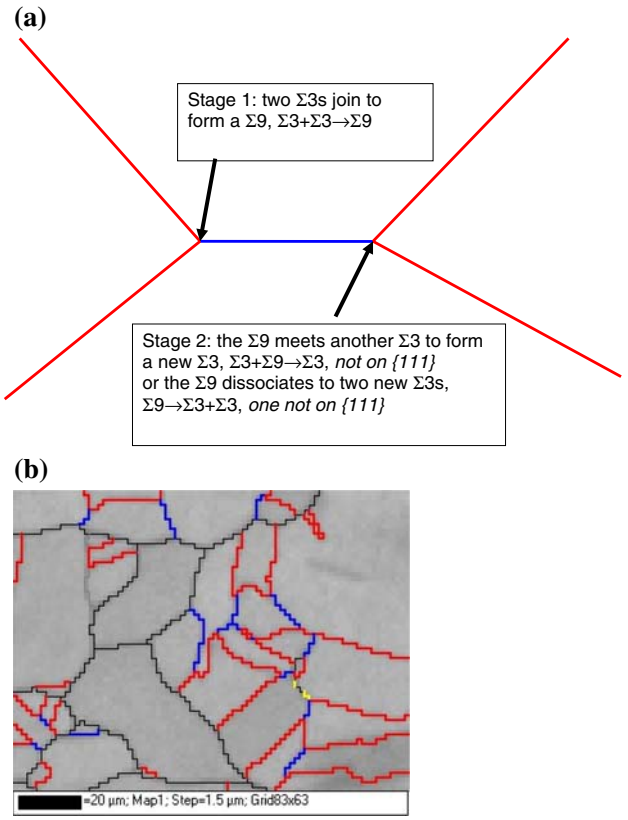

Fig. 7 (**a**) Schematic depiction of interactions between Σ3s to form a Σ9 'bridge'. Σ3s are red and the Σ9 linkage is blue. (**b**) Part of orientation map from the annealed specimen showing several examples of interactions between as depicted in (**a**)

subsequently encounter another, existing Σ3 which would produce a new Σ3 according to the reaction $\Sigma3 + \Sigma9 \rightarrow \Sigma3$ (stage 2). Hence the Σ9 forms a bridge between Σ3 couplets, which is illustrated schematically on Fig. 7a. As the Σ9 segment can have a variety of boundary planes (see the spread in the 40°/[110] section in Fig. 4) and usually a Σ9 boundary deviates from the exact Σ9 misorientation, the geometrical consequence is that the new Σ3 *would not be on {111}*. This is consistent with the experimental observations. In a similar manner, Σ27a boundaries can generate new Σ3s according to $\Sigma27 + \Sigma9 \rightarrow \Sigma3$. Interactions within the $\Sigma3^n$ family have been reported and analysed formally elsewhere [e.g., 19]. Σ9 boundaries could also dissociate to produce two Σ3s, one of which is incoherent. The driving force for this reaction is that the energy of both Σ3s is less than the Σ9. Such dissociation reactions have been observed in silicon [20].

There are many examples in the orientation maps of a Σ9 forming a bridge between two triple junctions where the other boundaries are Σ3s. Figure 7b is a portion of orientation map where several examples can be seen. All these interactions would require local migration of both Σ9s and also the mobile (incoherent) portion of Σ3s, and would have the result of destroying a proportion of the coherent Σ3 length and replacing it with incoherent segments. The length fraction of Σ9s does not increase during these interactions (in agreement with our experimental observations) because some of the interactions create Σ9s, and some of the interactions destroy them, thus creating a near-steady state. A similar sequence takes place during twinning-related GBE [21]. The mechanism described here presents a plausible explanation for the reduction in {111} plane density after annealing.

In summary, the effect of annealing on the evolution of the Σ3 population turned out to be more complex than expected, with the main feature being recombination

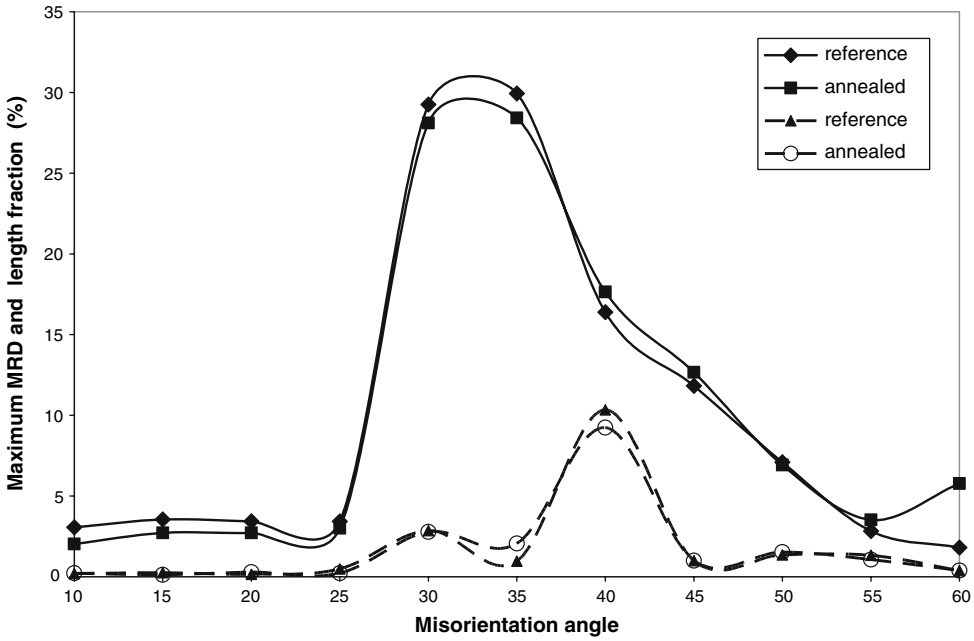

Fig. 8 Maximum MRD and misorientation length fraction of boundary as a function of misorientation angle on <110> for the reference and the annealed specimen. The MRD maxima are shown as full lines and the misorientation length fractions are shown as dashed lines

reactions with Σ9s. Boundary reorientation did not take place to any great extent in the Σ3 boundary population because the distribution in the reference sample, Fig. 6a, shows that the distribution of planes was already close to low energy, with many coherent twins present. This is in contrast to the previous work where the same annealing treatment was employed, because in that case the reference specimen had been processed in a different manner here, which produced many incoherent Σ3s [7].

Turning now to the non-Σ3 boundaries, there are significant changes in the distribution of boundary planes in the subset of boundaries which are misoriented on <110>. As described in the previous section, there is greater propensity for tilt boundaries after annealing, and there are subtle shifts in the distribution of population density along the [110] zone, which indicates a change in the plane population. Figure 8 shows for both specimens the distribution of maximum MRD as a function of misorientation angle about the [110] misorientation axis. The maximum MRD distributions peak at 30–35° and are skewed towards higher misorientation angles. Also displayed on Fig. 8 is the misorientation angle frequency distribution on the <110> axis. The highest peak is at 40°, which corresponds to the Σ9 population. A second, much smaller, peak occurs at 30° and corresponds to Σ27a. There is clearly much more of the misorientation population in the 40° section than elsewhere.

The actual planes along the [110] zone have changed after annealing, as shown in Fig. 4. We will consider in detail this change in the misorientation angle section that includes Σ9. Figure 9 shows in detail the boundary plane density distribution for the 40°/[110] section, which is close to Σ9, for the reference sample and the annealed sample. The density along the zone encompasses a number of possible ATGB plane combinations for Σ9 such as {111}/{115} and {211}/{552}. The {114} symmetrical tilt grain boundary (STGB) may also be present within this grouping. However, the most obvious and potentially the most significant change after annealing is the development of a well-defined maximum close to the other STGB, {221}, which is absent in the reference specimen. The significance of the presence of these ATGBs and STGBs in the Σ9 system is that they have lower energies than boundaries on irrational planes [6]. Many of the peaks along the [110] zone are overlapping so it is not possible to analyse most of them in detail, except to note that the detail in Fig. 9 confirms that the distribution of peaks on the [110] zone has changed as a result of annealing. The change in the Σ9 plane distributions profile is interpreted as a combination of local shifts in the boundary plane orientation plus the creation of new Σ9s according to the mechanism described above. Although part of this change may have been the result of geometrically necessary

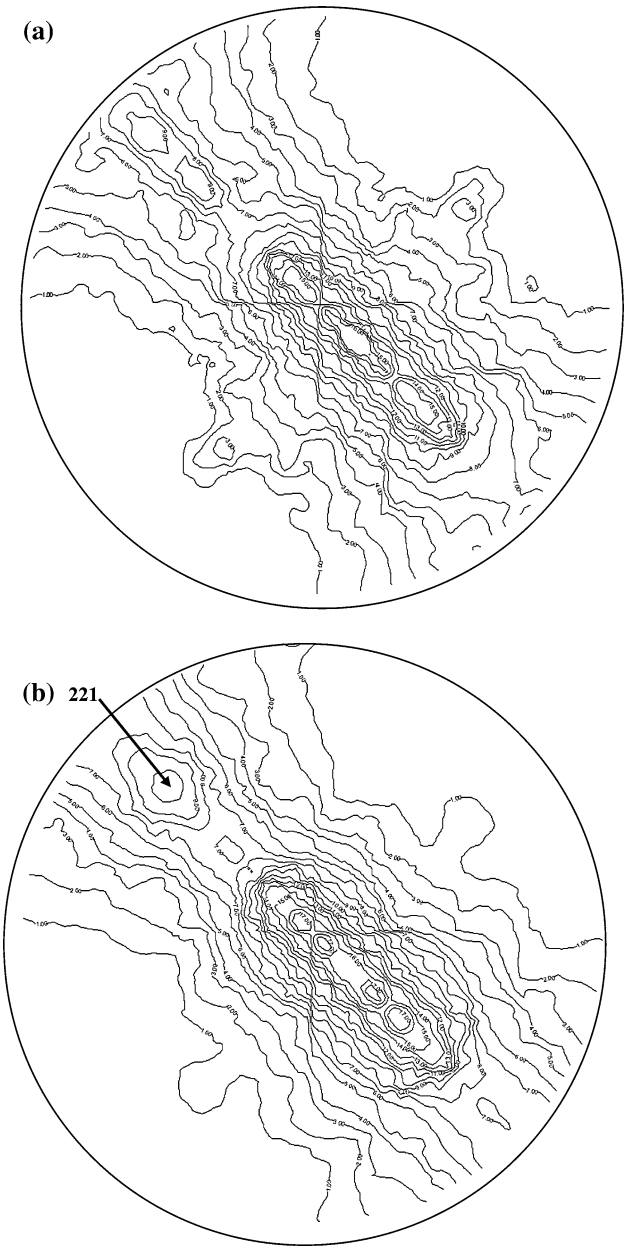

Fig. 9 Boundary plane density distribution shown as line contours in increments of 1× MRD for the 40°/[110] misorientation section. (**a**) reference sample (**b**) annealed sample. The location of {221} is marked on the annealed sample

bridges between Σ3s, the appearance of the {221} STGB after annealing suggests a concomitant reduction in energy associated with the modified plane distribution.

Apart from the regions of anomalous grain growth, there has been no sustained grain boundary migration during the long anneal. The migration of $\Sigma 3^n$ segments reported above are essentially intra-grain migration events. Neither has there been any significant changes in microtexture nor overall misorientation distribution. In consequence, any

change in the five-parameter distribution after annealing reflect mainly changes to the boundary plane population. This was the goal of the investigation, namely to anneal the samples at a temperature that was sufficiently low to discourage grain boundary migration and whole grain rotation, but yet would allow individual grain boundary plane reorientation. It is clear from the data shown here that a certain amount of boundary plane adjustments have taken place in the grain boundary network. The experimental evidence is the tendency for misorientations on [111] to become closer to exact (111) twist boundaries, and the tendency for misorientations on [110] to become closer to exact [110] tilt boundaries. The driving force for these changes has been the reduction of the overall grain boundary energy. Usually post recrystallisation anneals achieve grain boundary energy reduction by grain growth, i.e., reduction of grain boundary area, but in the present investigation the temperature was sufficiently low so as to suppress normal grain growth. Instead, boundary reorientation has been effective in these cases. We examined in detail only those sections of five-parameter space which corresponded to higher than average misorientation density. Changes in the boundary plane population may also have occurred in other misorientation ranges.

Finally, the results here have shown that low temperature annealing can provide a route to reduce the energy of the boundary network without grain growth. 'Grain boundary plane engineering' is therefore feasible, although the effect of the pinning restriction imposed by triple junctions on grain boundary reorientation has not yet been investigated. Given the simplicity of the processing, it is of interest to study further the effects of long duration, low temperature annealing on the energy minimisation of microstructure.

Conclusions

The effect of long duration annealing at 500 °C on the grain boundary population in copper has been studied in both a pre-annealed (reference) sample and a post-annealed sample, with particular focus on the boundary plane distribution. Both the microtexture and the proportions of Σ3, Σ9 and Σ27 boundaries remained static during the anneal, indicating that no new twinning had occurred. The Σ3, Σ9 and Σ27 length fractions were 61%, 6% and 3% respectively. There was anomalous grain growth in a few regions, whereas in all other regions the grain size remained static. The main findings of the investigation with regard to the boundary plane population were

- There was a strong maximum at {111} in the overall distribution, resulting mainly from the high fraction of coherent annealing twins in the Σ3 misorientation subset. Within this subset, the distribution about the {111} maximum indicated the presence of planes vicinal-to-{111} and asymmetrical tilt boundaries on the <110> zone. Within the general, non-Σ3 population there was a much weaker maximum at {111}.
- The density fraction of Σ3 boundary length on {111} planes had decreased after the long anneal. This was interpreted as a consequence of the intra-grain migration of incoherent Σ3s whereby an encounter between two Σ3s led to the formation of a Σ9 bridge, which in turn dissociated or encountered another Σ3 to produce a new, incoherent Σ3. Hence, there were more incoherent Σ3 segments after the long anneal than in the reference specimen.
- There was evidence, for those misorientation categories examined in detail, that some boundary plane segments had reoriented towards lower energy configurations during the long anneal. For boundaries disoriented on <110> a larger proportion of boundaries were tilt or near-tilt as a consequence of boundary reorientation during the long duration anneal. The distribution of planes on the tilt zone also had changed. For the case of Σ9 boundaries, the {221} symmetrical tilt boundary was present after annealing whereas it was absent in the reference specimen. Misorientations on <111> had become closer to exact twist.

Acknowledgements The authors acknowledge useful discussions and assistance with the five-parameter software from Professor G. Rohrer and Mr. H. Miller from Carnegie Mellon University, Pittsburgh, USA.

References

1. Randle V (2004) Acta Mater 52:4067
2. Kumar M, Schuh CA (eds) (2006) Viewpoint set no. 40, Scripta Mater. Grain boundary engineering, vol 54, p 961
3. Lin P, Palumbo G, Erb U, Aust KT (1995) Scripta Met Mater 33:1387
4. Janssens KGF, Olmsted D, Holm EA, Foiles SM, Plimpton SJ, Derlet PM (2006) Nat Mater 5:124
5. Wolf D (1990) Acta Metall Mater 38:791
6. Merkle KL, Wolf D (1992) Philos Mag 65A:513
7. Randle V, Davies P, Hulm B (1999) Philos Mag 79A:305
8. Lejcek P, Hofmann S, Paidar V (2003) Acta Mater 51:3951
9. Saylor DM, Adams BL, El-Dasher BS, Rohrer GS (2003) Metall Mater Trans 34A:1
10. Saylor DM, Morawiec A, Rohrer GS (2003) Acta Mater 51:3663
11. Saylor DM, El-Dasher BS, Rollett AD, Rohrer GS (2004) Acta Mater 52:3649

12. Randle V, Rohrer GS, Kim C, Hu Y (2006) Acta Mater 54:4 480
13. Brandon DG (1966) Acta Metall 14:1479
14. Fullman RL (1951) J Appl Phys 22:456
15. Sargent CM (1968) Trans Metall Soc AIME 242
16. Randle V, Davies H (2002) Ultramicroscopy 90:153
17. Wolf U, Ernst F, Muschik T, Finnis MW, Fischmeister HF (1992) Philos Mag A 66:991
18. Gindraux G, Form W (1973) J Inst Metal 101:85
19. Reed BW, Kumar M (2006) Scripta Mater 54:1029
20. Garg A, Clark WAT, Hirth JP (1989) Philos Mag 59:479
21. Randle V (1999) Acta Mater 47:4187